Molecular BioSystems

Accepted Manuscript

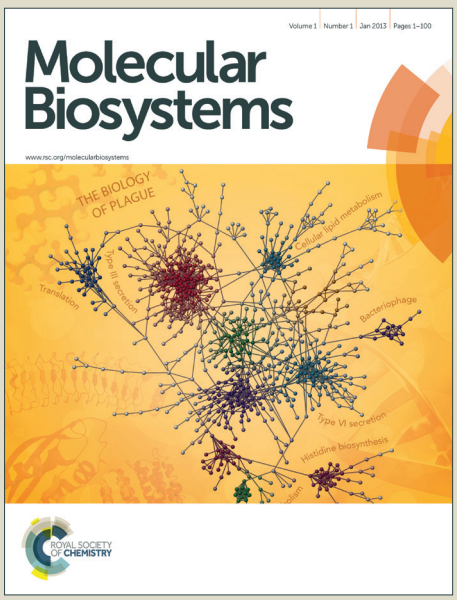

ROYAL SOCIETY OF CHEMISTRY

www.rsc.org/molecularbiosystems

Multi-spectroscopic and molecular modelling studies on the interaction of esculetin with calf thymus DNA

Tarique Sarwar, Mohammed Amir Husain, Sayeed Ur Rehman, Hassan Mubarak Ishqi and Mohammad Tabish*

Department of Biochemistry, Faculty of Life Sciences, A.M. University, Aligarh, U.P. 202002, India

Running title: Esculetin-DNA interaction

***Corresponding author:**
Department of Biochemistry
Faculty of Life Sciences
A.M. University, Aligarh
U.P. 202002, India
Email: tabish.bcmlab@gmail.com; Tel: +91-9634780818

No. of figures: 12
No. of Tables: 2

Conflict of Interest
The authors declare that there is no conflict of interest in this work.

Abstract

Understanding the interaction of small molecules with DNA has become an active research area at the interface between chemistry, molecular biology and medicine. Plant derived polyphenols possess diverse biological and pharmacological properties. Esculetin is a coumarin derivative polyphenolic compound having diverse pharmacological and therapeutic properties. However, its mode of interaction with DNA is still not well understood. In the present study, we have attempted to determine the mode of binding of esculetin with calf thymus DNA (Ct-DNA) through various biophysical techniques. Analysis of UV-visible absorbance spectra and fluorescence spectra indicates the formation of complex between esculetin and Ct-DNA. Binding constant was found to be $1.87 \times 10^4\ M^{-1}$. Thermodynamic parameters ΔG, ΔH, and ΔS at different temperatures indicated that hydrophobic interactions and hydrogen bonding played major role in the binding process. Several other experiments such as iodide induced quenching, competitive displacement studies with ethidium bromide, acridine orange and Hoechst 33258 suggested that esculetin possibly binds to the minor groove of the Ct-DNA. The strong dependence on ionic strength in controlling the binding of esculetin with Ct-DNA confirms the possibility of electrostatic interaction. These observations were further supported by DNA melting studies, viscosity measurements, CD spectral analysis and *in silico* molecular docking.

Keywords: Esculetin; calf thymus DNA; DNA binding; groove binding; DNA melting study; docking.

1. Introduction

There has been much interest in recent years in studying the interaction of small molecules with DNA due to their potential candidature as therapeutic agents against a number of diseases.[1] DNA is the pharmacological target of many drugs that are currently in clinical use or in advanced clinical trials.[2] Many clinically useful compounds against diseases such as cancer are known to exert their primary biological effects by modulating transcription or by interfering with replication.[3] Studying the interaction of small molecules with DNA is of current interest and has high significance. It provides assistance in the development of therapeutic drugs that may control the gene expression. New and more effective drugs can be designed which can recognize a specific site or conformation of DNA.[4] Three different non covalent modes through which small molecules interact with DNA are electrostatic interactions, intercalative binding and groove binding. Electrostatic binding occurs due to interaction between negatively charged DNA phosphate backbone and positively charged end of small molecules while intercalative binding occurs when small molecules intercalate within stacked base pairs thereby distorting the DNA backbone conformation.[5] Groove binding occurs due to hydrogen bonding or van der Waals interaction with nucleic acid bases and small molecules in the deep major groove or the shallow minor groove without causing any major distortion of the DNA backbone.[6] The availability of the genome sequence, well-studied three-dimensional structure of DNA and the predictability of their accessible chemical and functional groups make DNA as attractive drug target. However, the number of known drugs targeting DNA is still very limited compared to the drugs targeting proteins.[7]

Coumarins belong to a diverse group of naturally occurring plant derived polyphenols known as benzo-α-pyrones. A number of natural products with a coumarinic moiety have been reported to have various biological activities.[8] Esculetin (6,7- dihydroxy coumarin) is a coumarin derivative that can be isolated from many plants such as *Artemisia capillaries*, *Citrus limonia* and *Euphorbia lathyris*.[9,10] It has been shown to have multiple biological activities including the inhibition of xanthine oxidase activity, free radical scavenging activity, anti-inflammatory effects *in vivo*, neuroprotective effect, cancer chemoprevention, and anti-tumor activities.[11-16] Inspite of vast pharmacological properties of esculetin, its mode of binding with DNA has not been elucidated. It is thus pertinent to study the interaction of esculetin with DNA to reveal how this compound may be further modified to enhance its biological activities. The source being

natural dietary constituents, an understanding of the interactions of esculetin and other related derivatives has the potential to provide guidelines for the development of more potent compounds.

In the present study, we investigated the mode of binding of esculetin with DNA by using various spectroscopic techniques such as UV-visible absorbance and fluorescence spectroscopy. Various thermodynamic parameters for the interaction between esculetin and Ct-DNA were also calucated. In order to further confirm the mode of interaction between esculetin and DNA, melting study, viscosity measurement and circular dichroism spectroscopy were performed. *In silico* molecular docking further revealed the binding mode as well as relative binding energy of the complex formed between esculetin and DNA.

2. Experimental

2.1 Materials

Esculetin, Ct DNA, acridine orange (AO) and Hoechst 33258 were purchased from Sigma Aldrich, USA. Ethidium bromide (EB) was purchased from Himedia, India. Urea and potassium iodide (KI) were from Thermo Fisher Scientific, USA. All other chemicals and solvents were of reagent grade and were used without any further purification.

2.2 Sample preparation

Calf thymus DNA was dissolved in 0.1 M Tris-HCl buffer (pH 7.2) at room temperature. The purity of the DNA solution was checked by taking absorbance ratio $A_{260\ nm}/ A_{280\ nm}$. The concentrations of DNA solutions were determined by using the average extinction coefficient value of 6600 M^{-1} cm^{-1} of a single nucleotide at 260 nm.[17] The stock solution (10 mM) of esculetin was prepared in 0.1 mM NaOH and was diluted in distilled water for further use.

2.3 Instrumentations

All the UV-visible absorption spectra were recorded with Shimadzu dual beam UV-visible spectrophotometer UV-1800 (Japan) coupled with a thermostat bath, using a 1×1 cm quartz cuvettes. The fluorescence spectra and intensities were measured on a peltier fitted Shimadzu RF-5301PC spectroflurophotometer (Japan) equipped with xenon flash lamp using 1.0 cm quartz cells. The widths of both the excitation slit and emission slit were set at 5.0 nm.

2.4 Methods

2.4.1 UV spectroscopic method

The UV spectra of esculetin and esculetin-DNA complex were recorded in the wavelength range 240-300 nm. Experiment was carried out in presence of fixed concentration of esculetin (50 μM) and titrated with varying concentration of DNA (0-60 μM). The final volume of the reaction mixture was made to 3 ml by adding 10 mM Tris-HCl buffer (pH 7.2). Base line correction was was carried out using blank solution containing 60 μM of Ct-DNA in 10 mM Tris-HCl buffer.

2.4.2 Steady state fluorescence

Steady state fluorescence emission spectra of esculetin were recorded in the range of 410 to 560 nm upon excitation at 268 nm. The change in fluorescence intensity was observed by titrating the fixed amount of esculetin (50 μM) with varying concentration of Ct-DNA from 0 to 45 μM at different temperatures (294 K, 304 K, and 318 K). The final volume of the reaction mixture was made to 3 ml by adding 10 mM Tris-HCl buffer (pH 7.2).

2.4.3 Potassium iodide (KI) quenching method

It was performed in presence and absence of Ct-DNA. Esculetin (50 μM) was taken into a 3 ml reaction mixture containing 10 mM Tris-HCl (pH 7.2) and emission spectra were recorded after adding increasing concentration of of KI (0-30 mM). In another set, similar experiment was done in presence of 50 μM of Ct-DNA. Emission spectra in the range of 410-560 nm were recorded upon excitation at 268 nm.

2.4.4 Competitive displacement assays

EB displacement assay was performed as reported earlier (Morgan et al., 1979). This assay was carried out by adding EB to Ct-DNA solution. The concentration of EB and Ct-DNA were 5 μM and 50 μM respectively and this was titrated with varying concentration of esculetin from 0 to 80 μM. The EB-Ct-DNA complex was excited at 476 nm and emission spectra were recorded between 535 nm to 675 nm.

AO displacement assay was carried similar to EB displacement. AO-Ct-DNA complex containing 5μM of AO and 50 μM of Ct-DNA was excited at 480 nm and fluorescence emission spectra was recorded between 490-600 nm by titrating AO-Ct-DNA complex by varying concentration of esculetin from 0 to 80 μM.

Hoechst 33258 displacement assay was also done similar to EB and AO displacement assays. Hoechst-Ct-DNA complex containing 5μM of Hoechst and 50 μM of Ct-DNA was excited at 343 nm and fluorescence emission spectra were recorded between 375-600 nm by

titrating with increasing concentration of esculetin from 0 to 80 μM. The final volume of the reaction mixture in all the above experiments was made to 3 ml by adding 10 mM Tris HCl buffer (pH 7.2).

2.4.5 Effect of ionic strength

Effect of ionic strength on interaction between esculetin and Ct-DNA was studied by varying the concentration of NaCl between 0-15 mM in total volume of 3 ml containing 50 μM esculetin, 50 μM Ct-DNA and 10 mM Tris-HCl (pH 7.2). Excitation was done at 268 nm and emission spectra were recorded between 375-575 nm.

2.4.6 DNA melting studies to study the change in *T*m

DNA melting experiments were carried out by monitoring the absorption of Ct-DNA (50 μM) at 260 nm in the absence and presence of esculetin (50 μM) at various temperatures by a spectrophotometer attached with a thermocouple. The volume of the sample was made up to 3 ml using 10 mM Tris-HCl buffer (pH 7.2). The absorbance was then plotted as a function of temperature ranging from 25°C to 100°C. The DNA melting temperature (*T*m) was determined as the transition midpoint.

2.4.7 Viscosity Measurement To elucidate the binding mode of esculetin, viscosity measurements were carried out by keeping DNA concentration constant (50 μM) and varying the concentration of esculetin. Viscosity measurements were carried out with an Ubbelohde viscometer suspended vertically in a thermostat at 25^0C (accuracy $\pm$0.1^{o}C). The flow time was measured with a digital stopwatch, and each sample was tested three times to get an average calculated time. The data were presented as $(\eta/\eta_0)^{1/3}$ versus concentrations of DNA/esculetin ratio, where η and η_0 are the viscosity of esculetin in the presence and absence of DNA respectively.[18]

2.4.8 CD studies

CD spectra of Ct-DNA (30 μM) alone and with increasing concentration of esculetin (0-60 μM) were recorded using Applied Photophysics CD spectrophotometer (U.K.; model CIRASCAN) equipped with a peltier temperature controller to keep the temperature of the sample constant at 25^0C. All the CD spectra were recorded in a range from 220 nm to 310 nm with a scan speed of 200 nm/min with a spectral band width of 10 nm. Average of four scans was taken in all the experiments. Background spectrum of buffer solution (10 mM Tris-HCl, pH 7.2) was subtracted from the spectra of DNA and esculetin-DNA complex.

2.4.9 Molecular Docking

The molecular docking studies were performed by using HEX 6.3 software HEX is an interactive molecular graphics program for calculating and displaying feasible docking modes of DNA.[19] Structure of the B-DNA dodecamer d(CGCGAATTCGCG)2 (PDB ID: 1BNA) was downloaded from the protein data bank (http://www.rcsb.org./pdb). Both the ligand and the receptor are put in PDB format. The parameters used for docking include: correlation type – shape only, FFT mode – 3D, grid dimension – 0.6, receptor range- 180, ligand range-180, twist range-360, distance range-40. Mol file of esculetin was obtained from http://pubchem.ncbi.nlm.nih.gov/ and converted into PDB format using Avagadro's 1.01. Visualization of the docked poses was done by Py-Mol molecular graphic program available at http://pymol.sourceforge.net/.[17]

Since the docking force-fields may not be fully reliable, molecular dynamics simulation of docked pose of esculetin-DNA complex having minimum energy was performed for a short time using AMBER, present in MDweb (http://mmb.irbbarcelona.org/MDWeb) to check the RMSD fluctuations.[20,21] The complex was first soaked in a box of water molecule. The total number of water molecules added was 2250. The charges were neutralized by the addition of 29 Na+ and 7 Cl- ions to maintain neutrality.

3. Results and discussions

3.1 Non-covalent interaction of esculetin with DNA

3.1.1 UV-visible spectroscopy

UV-visible absorption spectroscopy is the most widely used method in detecting the interaction of small molecules with DNA and formation of their complex. Generally, changes in the absorbance and/or in the position of peak is observed, when a small molecule interacts with DNA and forms a complex.[22] Strength of interaction is correlated with the magnitude of changes in absorbance or shifting in the peak position.[23,24] Small molecules binding with DNA through intercalation usually results in hypochromism with red shift.[25] In case of groove binding or electrostatic attraction between small molecules and DNA, hyperchromism with no or little red shift is observed, that reflects the corresponding changes in the conformation and structure of the DNA. The UV absorption spectra of esculetin with increasing concentration of Ct-DNA are shown in Fig. 1B. In absence of DNA, esculetin shows maximum absorbance at 268 nm. On subsequent addition of Ct-DNA, hyperchromism is observed, indicating the formation of

complex between esculetin and Ct-DNA. However, red shift was not observed, suggesting groove binding and/or electrostatic interaction rather than intercalative mode of interaction between esculetin and Ct-DNA.

3.1.2 Steady state fluorescence

Fluorescence emission spectroscopy provides additional information regarding the binding mode of small molecules with.[26] Since, the endogenous fluorescence property of DNA is poor, fluorescence spectra of esculetin is studied in all subsequent fluorescence studies. Fig. 2 shows the fluorescence emission spectra of esculetin with emission maxima at 468 nm after excitation at 268 nm. On subsequent addition of Ct-DNA there is a gradual quenching of the fluorescence intensity without any significant change in emission maxima which is a direct evidence for the interaction between esculetin and Ct-DNA.[27]

In order to study the quenching process and to distinguish the possible quenching mechanism, quantitative estimation in terms of the fluorescence change was performed using the Stern-Volmer equation.[28]

$$F_0/F = 1 + Ksv\,[Q] \qquad (1)$$

where F_0 and F are the fluorescence intensities of esculetin in the absence and presence of Ct DNA (Q), respectively. Ksv is the Stern-Volmer quenching constant which is considered as a measure of efficiency of fluorescence quenching by DNA. As shown in Fig. 3, Ksv values were calculated from the slope of the Stern-Volmer plot at different temperatures (294 K, 304 K and 318 K) using equation (1). Ksv values were in the range of 0.72-1.87 × 10^4 and are listed in Table 1, which are consistent with groove binders.[29] Thus, esculetin is suggested to interact with Ct-DNA through non-covalent interaction possibly by groove binding mode.

A linear Stern-Volmer plot as obtained in the Fig. 3 suggests that only one type of binding or quenching process occurs, either static or dynamic quenching which can be differentiated using following equation.[30]

$$kq = Ksv/\tau_0 \qquad (2)$$

where, kq is the apparent bimolecular quenching rate constant, τ_0 is the fluorescence lifetime of the biomolecule in absence of quencher which is around 10^{-8} s.[31] kq of biomolecules is known to be around 2.0×10^{10} $M^{-1}s^{-1}$. kq calculated using equation (2) was found to be in the range of 0.72-1.87 × 10^{12} $M^{-1}s^{-1}$ at different temperatures (Table 1) which is much higher than bimolecular quenching rate constant.[31] By analyzing the Ksv values at different temperatures, dynamic and

static quenching can be differentiated. In case of static quenching a decrease in values is observed with increasing temperature while reverse is observed in case of dynamic quenching.[28] In case of esculetin-DNA interaction, a gardual decrease in the *Ksv* values with increase in temperature was observed (Table 1). Thus, confirming that the quenching process is static rather than dynamic.

3.1.3 Calculation of binding constant

Fluorescence titration data at different temperatures was used to calculate various binding parameters of esculetin-DNA interaction using modified Stern-Volmer equation.[32]

$$\log[(F_0 - F)/F] = \log K + n\log[Q] \quad (3)$$

where, F_0 and F are the fluorescence emission intensities of esculetin in absence and presence of Ct-DNA, n is the number of binding sites and K is the binding constant. Plot of $\log[(F_0/F)/F]$ *versus* log[DNA] was obtained and the intercept of this plot corresponds to log$K$ (Fig. 4). As mentioned in Table 1, value of K was calculated to be 4.49×10^4 M^{-1} at 294 K which decreases with increasing temperature. Value of n was obtained from the slope of the above mentioned plot which was found to be close to one at different temperatures.

3.1.4 Determination of thermodynamics parameters

The major forces acting during non-covalent interactions between small molecules and macromolecules such as protein and DNA are electrostatic forces, hydrogen bonds, van der Waals forces and hydrophobic interactions.[33] Thermodynamic parameters such as enthalpy change (ΔH), entropy change (ΔS) and free energy change (ΔG) are very important in defining these binding forces. In case of esculetin-DNA interaction these thermodynamic parameters were calculated with the help of following equations.[34]

$$\log K = -\Delta H/(2.303RT) + \Delta S/(2.303R) \quad (4)$$

$$\Delta G = \Delta H - T\Delta S \quad (5)$$

Here K and R are the binding constant and gas constant respectively. The values of ΔH and ΔS were evaluated from the slope and intercept of van't Hoff plot (Fig. 5). ΔG was calculated from equation (5) and is summarized in Table 1 along with ΔH and ΔS. The negative value of ΔG means that the binding process is favourable and spontaneous. By calculating the values of ΔH and ΔS, type of interaction between small molecule and DNA can be identified. In our study the values calculated for ΔH and ΔS are -3.77 kcal/mol and +8.51 cal/mol respectively. The positive value of ΔS is frequently regarded as evidence for a hydrophobic interaction.[31] The negative ΔH

value showed that the binding process is mainly enthalpy driven and by means of hydrogen binding interactions.[35] Thus, both hydrophobic interactions and hydrogen bonding played a major role in the binding of esculetin to DNA and contributed to the stability of the complex.[22]

3.2 Esculetin binds to the minor groove of DNA

3.2.1 KI Quenching Study

In order to elucidate the mode of binding of esculetin with DNA, its fluorescence quenching in the absence and presence of Ct-DNA was studied using potassium iodide as a quencher.[36] Iodide ions are negatively charged quencher that can effectively quench the fluorescence of small molecules in an aqueous medium. It is well established that DNA contains negatively charged phosphate backbone and so, it is expected to repel anionic quenchers. Therefore, fluorescence intensity of an intercalating small molecule is well protected from being quenched as the approach of anionic quenchers towards fluorophore is restricted.[37] However, groove binding provides little protection for the fluorophore as they are exposed to the external environment and iodide anions can readily quench their fluorescence even in the presence of DNA.[19] Accessibility of small molecules to anionic quencher in free medium as well as in presence of DNA was studied using Stern-Volmer equation and *Ksv* was calculated. Fig. 6 shows the Stern-Volmer plot for fluorescence quenching of esculetin by KI in absence and presence of Ct-DNA. *Ksv* of free esculetin by iodide anions was 9.25 M^{-1} and in the presence of Ct-DNA, *Ksv* was 8.13 M^{-1}. A very little decrease in *Ksv* was observed when esculetin is bound to Ct-DNA, which indicatede that the bound esculetin molecules have not intercalated into the base pairs of the DNA. Some reports suggest a slight protection of drug by DNA even in the case of groove binding, but this protection is very less as compared to intercalation.[38] Thus, we speculated that groove binding mode of interaction occurs between esculetin and Ct-DNA.

3.2.2 Competitive displacement assays

Various well known DNA binding dyes whose binding modes have already been established are used to decipher the mode of drug-DNA interaction. In competitive displacement assays, any small molecule that replaces the dye already bound to DNA will interact with DNA in the same mode as the replaced dye. The change in fluorescent behaviour of drug-DNA system on binding of small molecules, gives valuable information regarding the mode of binding.[19]

EB is one of the most sensitive fluorescence probes having a planar structure that binds to DNA via intercalative mode. EB shows weak fluorescence in the solvent. However, its

fluorescence intensity is increased in the presence of DNA as it gets intercalated within DNA base pairs.[39] In EB displacement assay, any molecule that binds to DNA via same mode as EB, will replace EB from DNA helix and result in decrease in the fluorescence intensity of EB-DNA system. The extent of fluorescence quenching of EB-DNA system can be used to determine the extent of intercalation between the molecule and DNA.[33,40] Fig. 7A shows the fluorescence emission spectra of EB-DNA. On subsequent addition of esculetin there was no significant decrease in the fluorescence intensity, suggesting that esculetin binds to DNA in non-intercalative mode.

In order to further rule out the possibility of intercalative mode of binding of esculetin with DNA, AO displacement assay was carried out. It has been proved that AO is a sensitive fluorescence probe having a planar aromatic structure that binds to DNA by an intercalative mode.[41] The fluorescence intensity of AO-DNA is remarkably stronger than AO alone. However, when small molecules replace AO after intercalation into DNA base pairs, the fluorescence intensity of AO-DNA system decreases remarkably. Fig. 7B shows the emission spectrum of AO-DNA system. It is observed that the fluorescence intensity of AO-DNA is not decreased significantly on subsequent addition of esculetin, indicating that esculetin is not able to replace AO. This result again confirmed that esculetin does not bind to DNA by intercalative mode. Thus, to confirm the possibility of minor groove binding another dye displacement assay using known minor groove binder was performed.

Hoechst 33258 fluorescent dye is a known minor groove binder of the double helical DNA.[42] Hoechst produces weak fluorescence in aqueous solution. However, in presence of DNA, fluorescence intensity of Hoechst 33258 is enhanced substantially.[43] Any small molecule that binds to DNA via same mode as Hoechst will replace the Hoechst from the minor groove of the DNA helix and will result in the quenching of fluorescence intensity of Hoechst-DNA system.[19] Fig. 7C shows the change in fluorescence spectra of Hoechst-Ct-DNA system on addition of esculetin. On subsequent addition of esculetin there was significant decrease in the fluorescence intensity of Hoechst-DNA system, supporting the view that esculetin interacted with DNA via minor groove binding after replacing Hoechst.

The quenching of EB, AO and Hoechst bound to Ct-DNA by esculetin was calculated in terms of *Ksv* from the Stern-Volmer plot as shown in the Fig. 7D using equation 1.[44] *Ksv* values are 1.15×10^3 M^{-1}, 0.74×10^3 M^{-1} and 5.38×10^3 M^{-1} in case of EB, AO and Hoechst respectively

(Table 2). It is evident that *Ksv* value in case of Hoechst is much higher as compared to EB and AO. Thus, it may be concluded that esculetin binds to Ct-DNA at the minor groove after replacing Hoechst from it.

3.2.3 Effect of ionic strength

The effect of the ionic strength is also an efficient method to distinguish the binding mode between small molecules and DNA. It is apparent that both intercalative and groove bindings are closely related to the DNA double helix, but the electrostatic binding can take place from outside the helix. To study the role of electrostatic interaction in esculetin-DNA binding, NaCl was used. When NaCl exists in the system, the electrostatic repulsion between the negatively charged phosphate backbone on adjacent nucleotides is reduced with increasing concentration of Na^+. Thus, electrostatic interactions are shielded in the presence of Na^+ ions and the DNA chains will be tightened.[45] In case of groove binding, a small molecule binds in the groove of DNA duplex and exposes much to the surroundings than intercalation do.[46] Thus, the groove bound molecules can be easily released from helix by increasing the ionic strength whereas it is difficult for intercalatively bound molecules.[37] The effect of ionic strength on the fluorescence spectra of esculetin-Ct-DNA system was observed by the addition of NaCl as shown in Fig. 8. With increasing concentration of NaCl, fluorescence intensity of esculetin-Ct-DNA system was substantially enhanced. This may be due to the weakening of electrostatic attraction between esculetin and Ct-DNA surface and subsequent release of groove-bound esculetin from the DNA helix. The strong dependence of the binding on the ionic strength clearly indicated that binding of esculetin to DNA is predominantly controlled by electrostatic interaction which has already been confirmed above. These observations are consistent with groove binding rather than intercalation into the helix.[37]

3.2.4 DNA melting studies

The double-helical structure of DNA is remarkably stable due to hydrogen bonding and base stacking interactions. Upon increasing the temperature, the double helix dissociates to single strands due to weakening of various binding forces. The temperature at which half of the DNA double helix is denatured into single stranded DNA is known as the melting temperature (*T*m), and is strongly related to the stability of the double-helical structure.[47] Interactions of small molecules with DNA are known to influence *T*m. Intercalative mode of binding of small molecules can further stabilize the DNA double helical structure and increases the *T*m by about

5–8 °C. But non-intercalative binding such as groove binding or electrostatic binding causes less or no significant increase in *T*m.[37] The value of *T*m for Ct-DNA in absence and presence of esculetin was determined from the plot of $A/A_{25°C}$ versus Temperature by monitoring the absorbance at 260 nm as the transition midpoint of the melting curve (Fig. 9). Here $A_{25°C}$ is the absorbance at 25°C and A is the absorbance at increasing temperature ranging from 25°C to 100°C. Under the experimental conditions, value of *T*m for Ct-DNA alone was 67.0 ± 1°C, while in the presence of esculetin, it was found to be 69.3 ± 1°C. The observed change in *T*m was very less, supporting the above observations that the binding mode was non-intercalative. The slight increase in *T*m is presumably due to change in the conformation of DNA as a result of groove binding of esculetin with DNA.

3.2.5 Viscosity measurements

To further confirm the binding mode of between esculetin and Ct-DNA, viscosity measurement study was employed. Viscosity measurement is sensitive to change in length of DNA and is regarded as the least ambiguous and critical test for determining the binding mode in solution.[48] A classical intercalator causes a significant increase in the viscosity of DNA solution due to increase in separation of base pairs at the intercalation sites leading to overall increase in the length of the DNA.[17] On the other hand, small molecule that binds exclusively in the DNA grooves or through electrostatic interaction under the same conditions, causes less or no changes in the viscosity of the DNA solution.[19,49] A viscosity plot of $(\eta/\eta_o)^{1/3}$ versus [esculetin]/[DNA] was obtained to study any change in the viscosity of Ct-DNA solution in presence of esculetin. As shown in Fig. 10, with continuous addition of esculetin to Ct-DNA solution, very little increase in viscosity was observed which was not as pronounced as observed for classical intercalators. Thus, confirming that esculetin interacts with minor groove of DNA and ruling out the possibility of intercalation.

3.2.6 CD studies

CD spectroscopy is very sensitive to the changes in the secondary structure of bio-macromolecules and thus has been employed to detect changes in the secondary structure of DNA on interaction with small molecules.[50] Various changes in CD spectra of DNA are linked to the corresponding changes in DNA structure.[51] Non covalent DNA-drug interactions affect the DNA structure leading to altered CD spectral behaviour.[17,52] The CD spectrum of Ct-DNA exhibits a positive band at ~275 nm due to base stacking and a negative band at ~245 nm due to

the right-handed helicity of B-DNA form which are sensitive to interactions with small molecules.[53] Groove binding and electrostatic interaction of small molecules show less or no perturbation on the base stacking and helicity bands, whereas intercalation alters the intensities of both the bands significantly, thus stabilizing the right-handed B conformation of DNA.[54] As shown in the Fig. 11, on subsequent addition of esculetin to Ct-DNA, the CD spectrum of B-DNA is not perturbed. Thus, there may be a possibility that esculetin binds to DNA primarily by a groove mode of binding. However, a little change in the intensities of bands at 245 nm and 275 nm may be due to certain conformational changes, such as the conversion of DNA from a more B-like to a more A-like structure.

3.2.7 Molecular docking

Docking studies provide some insight into the interactions between the macromolecule and ligand, which can corroborate the experimental results. Although the crystal structure of the complex can represent specific details of the interactions, general observations may be obtained from docking studies. Molecular docking technique is an attractive scaffold to understand the drug-DNA interactions for the rational drug design and discovery.[55] Molecular modeling allows the flexibility within the ligand to be modelled and can utilize more detailed molecular mechanics to calculate the energy of the ligand in the context of the putative active site. In our experiment, structure of esculetin was made flexible to attain different conformations in order to predict the binding mode with DNA duplex of sequence $d(CGCGAATTCGCG)_2$ dodecamer (PDB ID:1BNA). The energetically most favourable conformation of the docked structure was analysed. Fig. 12, clearly indicated that esculetin fits into the curved contour of the targeted DNA in the minor groove showing the possibility of hydrogen bonding with the base pairs of dodecamer.[56] The resulting minimum relative binding energy of docked esculetin-DNA complex was found to be -3.60 kcal/mol. Relative binding energy for other docked poses and structures are provided in the supplementary information. The energy obtained from docking studies was comparable with the experimental results. Irrespective of the absence of any net positive charge on esculetin, negative value of the binding energy indicated a higher binding potential of the esculetin with DNA.

To check the stability of the esculetin-DNA complex, molecular dynamics simulation was performed. The average RMSD values were found to be low (0.14 Å to 0.33 Å) during the

course of the simulation. The result clearly shows that the stability of the complex is evenly distributed over the whole structure indicating no significant change.[57]

Thus, we conclude that there is a mutual complement between spectroscopic studies and molecular docking techniques, which can substantiate our experimental results and at the same time provide further evidence of groove binding.

4. Conclusion

In conclusion, we have studied the interaction of esculetin with Ct-DNA using various biophysical techniques. Through the analysis of UV absorbance spectra and steady state fluorescence, formation of esculetin-DNA complex was confirmed. Various thermodynamic parameters revealed that the binding process was spontaneous involving hydrophobic interation and hydrogen bonding. KI quenching study and competitive displacement assays with EB, AO and Hoechst 33258 revealed that esculetin interacts with DNA through groove binding mode. This was further confirmed by DNA melting studies, CD spectral analysis and viscosity measurement. Effect of ionic strength again confirmed the involvement of electrostatic interaction between esculetin and Ct-DNA. *In silico* molecular docking further confirmed that esculetin binds to the minor groove of the DNA with relative binding energy of -3.6 kcal/mol. Our results provide valuable information regarding drug-DNA interactions, which may be useful for the rational drug designing having greater clinical efficacy.

Acknowledgements

We are thankful to UGC, New Delhi, for the award of UGC-MANF to TS & MAH & CSIR fellowships to SR & HMI. We thank A.M.U. Aligarh for providing them the necessary facilities. We also thank University Grants Commission, New Delhi for providing financial assistance to the Department of Biochemistry under the DRS-III program and Advance Instrumentation Research Facility, Jawaharlal Nehru University, New Delhi, for carrying out some experiments.

References

1. N. Shahabadi and M. Maghsudi, *Mol Biosyst.*, 2014, **10**, 338–347.
2. A. Opar, *Nat Rev Drug Discov.*, 2009, **8**, 437–438.
3. M.H. Pan and C.T. Ho, Chem Soc Rev., 2008, **37**, 2558–2574.
4. S. Sobha, R. Mahalakshmi and N. Raman, *Spectrochim Acta A Mol Biomol Spectrosc.*, 2012, **92**, 175–183.
5. K.E. Erkkila, D.T. Odom and J.K, Barton, *Chem Rev.,* 1999, **99**, 2777–2795.
6. G. Barone, A. Terenzi, A. Lauria, A.M. Almerico, J.M. Leal, N. Busto and B. García *Coordination Chemistry Reviews*, 2013, **257**, 2848–2862.
7. H.M. Berman, J. Westbrook, Z. Feng, G. Gilliland, T.N. Bhat, H. Weissig, I.N. Shindyalov and P.E. Bourne, *Nucleic Acids Res.,* 2000, **28**, 235–242.
8. C.R. Wu, M.Y. Huang, Y.T. Lin, H.Y. Ju,, and H. Ching, *Food Chemistry,* 2007, **104**, 1464-1471.
9. K.C. Fylaktakidou, D.J. Hadjipavlou–Litina, K.E. Litinas and D.N. Nicolaides, *Current Pharmaceutical Design,* 2004, **10**, 3813–3833.
10. Y. Masamoto, H. Ando, Y. Murata, Y. Shimoishi, M. Tada, K. Takahata, *Biosci Biotechnol Biochem.,* 2003, **67**, 631–634.
11. D. Egan, R. O'Kennedy, E. Moran, D. Cox, E. Prosser and R.D. Thornes, *Drug Metabolism Reviews*, 1990, **22**, 503–529.
12. C.R. Lee, E.J. Shin, H.C. Kim, Y. S. Choi, T. Shin and M.B. Wie, *Lab. Anim. Res.*, 2011, **27**, 259–263.
13. O.S. Kwon, J.S. Choi, M.N. Islam, Y.S. Kim and H.P. Kim, *Arch. Pharm. Res*., 2011, **34**, 1561–1569.
14. C. Wang, A. Pei, J. Chen, H. Sun, M.L. Yu, C.F. Liu, X. Xu, *J Neurochem.,* 2012, **121**, 1007–1013.
15. S.Y. Lee, T.G. Lim, H. Chen, S.K. Jung, H.J. Lee, M.H. Lee, D.J. Kim, A. Shin, K.W. Lee, A.M. Bode, Y.J. Surh, Z. Dong, *Cancer Prev Res*., 2013, **6**, 1356–1364.
16. S.H. Kok, C.C. Yeh, M.L. Chen and M.Y. Kuo, *Oral Oncol.*, 2009, **45**, 1067–1072.
17. M.A Husain, Z. Yaseen, S.U. Rehman, T. Sarwar, M. Tabish, *FEBS J*., 2013, **280**, 6569–6580.
18. G. Cohen and H. Eisenberg, *Biopolymers,* 1969, **8**, 45–55.

19. S.U. Rehman, Z. Yaseen, M.A. Husain, T. Sarwar, H.M. Ishqi and M. Tabish, *PLoS ONE,* 2014, *9,* e93913.
20. D.A. Case, T.E. Cheatham 3rd, T. Darden, H. Gohlke, R. Luo, K.M. Merz Jr, A. Onufriev, C. Simmerling, B. Wang and R.J. Woods, *J Comput Chem.,* 2005, **26,** 1668-1688.
21. A. Hospital, P. Andrio, C. Fenollosa, D. Cicin-Sain, M. Orozco and J.L. Gelpí, *Bioinformatics,* 2012, **28**, 1278-1279.
22. G. Zhang, P. Fu, L. Wang, M. Hu, *J Agric Food Chem.,* 2011, **59**, 8944–8952.
23. J. Jaumot and R. Gargallo, Curr. Pharmaceut. Des. 2012, **18**, 1900–1916.
24. H. Sun, J. Xiang, Y. Liu, L. Li, Q. Li, G. Xu and Y. Tang, *Biochimie,* 2011, **93**, 1351–1356.
25. M. Rahban, A. Divsalar, A.A. Saboury and A. Golestani, *J. Phys.Chem. C,* 2010, **114**, 5798−5803.
26. B. Yang, J. Feng, Y. Li, F. Gao, Y. Zhao and J. Wang, *J Inorg Biochem.,* 2003, **96**, 416–424.
27. H.Y. Zou, H.L. Wu, Y. Zhang, S.F. Li, J.F. Nie, H.Y. Fu and R.Q. Yu, *J Fluoresc.,* 2009, **19**, 955–966.
28. J.R. Lakowicz, *Springer Publications,* New York, 2006, **3rd edn**.
29. C.V. Kumar, E.H.A. Punzalan and W.B. *Tetrahedron,* 2000, **56**, 7027–7040.
30. P. Kalaivani, R. Prabhakaran, M.V. Kaveri, R. Huang, R.J. Staples and K. Natarajan, *Inorganica Chimica Acta,* 2013, **405**, 415–426.
31. X. Ling, W. Zhong, Q. Huang and K. Ni, *J Photochem Photobiol B*. 2008, **93**, 172–176.
32. L.S. Lerman, *Journal of Molecular Biology,* 1961, **3**,18-30.
33. P.D. Ross and S. Subramanian, *Biochemistry,* 1981, **20**, 3096-3102.
34. R.R. Pulimamidi, R. Nomula, R. Pallepogu and H. Shaik, *Eur J Med Chem.*, 2014, **79**, 117–27.
35. J.L.Yuan, H. Liu, X.Kang, Z.Lv and G.L. Zou, J. Mol. Struct. 2008, 891, 333–339.
36. X. Zhou, G. Zhang, L.Wang. Int J Biol Macromol., 2014, **67,** 228-237.
37. C.V. Kumar, R.S. Turner and E.H. Asuncion, *J Photochem Photobiol A,* 1993, **74**, 231–238.

38. W.Y. Li, J.G. Xu, X.Q. Guo, Q.Z. Zhu and Y.B. Zhao, *Spectrochim. Acta A,* 1997, **53**, 781–787.
39. J. Olmsted and D.R. Kearns, *Biochemistry,* 1977, **16**, 3647–3654.
40. H. Wu, F. Jia, F. Kou, B. Liu, J. Yuan and Y. Bai, *Tran. Met. Chem.*, 2011, **36**, 847–853.
41. M.B. Lyles and I.L. Cameron, Biophys Chem., 2002, **96**, 53–76.
42. R. Kakkar, R. Garg and Suruchi, J Mol Struct Theochem., 2002, **579**,109–113.
43. Y. Guan, W. Zhou, X. Yao, M. Zhao and Y. Li, Anal. Chim. Acta, 2006, **570**, 21–28.
44. T. Sarwar, S.U. Rehman, M.A. Husain, H.M. Ishqi and M. Tabish, *Int. J. Biol. Macromol.*, 2014, doi:10.1016/j.ijbiomac.2014.10.017 In press.
45. J.B. Lepecq and C. Paoletti, *J Mol Biol.* 1967, **27**, 87–106.
46. H. Sun, J. Xiang, Y. Liu, L. Li, Q. Li, G. Xu and Y. Tang, *Biochimie*, 2011, **93**, 1351–1356.
47. U. Chaveerach, A. Meenongwa, Y. Trongpanich, C. Soikum, and P. Chaveerach, *Polyhedron,* 2010, **29**, 731–738.
48. C.S. Liu, H. Zhang, R. Chen, X.S. Shi, X.H. Bu and M. Yang, *Chem Pharm Bull.,* 2007, **55**, 996–1001.
49. G. Zhang, L. Wang, X. Zhou, Y. Li and D. Gong, *J Agric Food Chem.,* 2014, **62**:991-1000.
50. A.I. Holm, L.M. Nielsen, S.V. Hoffmann and S.B. Nielsen, *Phys. Chem. Chem. Phys.,* 2010, **12**, 9581–9596.
51. A.K Patra, M. Nethaji and A.R. Chakravarty, *J Inorg Biochem*., 2007, **101**, 233–244.
52. G. Zhang, X. Hu and J. Pan, *Spectrochim Acta A Mol Biomol Spectrosc.*, 2011 **78**,687–694.
53. M.P. Uma and M.J. Palaniandavar, *Inorg Biochem,* 2004, **98**, 219−230.
54. Y. Li, G. Zhang, J. Pan and Y. Zhang, *Sensors and Actuators B: Chemical,* 2014, **191,** 464–472.
55. R. Rohs, I. Bloch, H. Sklenar and Z. Shakked, *Nucleic Acids Res.,* 2005, **33**, 7048–7057.
56. R. Filosa, A. Peduto, S.D. Micco, Pd. Caprariis, M. Festa, A. Petrella, G. Capranico and G. Bifulco, *Bioorg Med Chem,* 2009, **17**, 13–24.
57. M. Walker, A.J. Harvey, A. Sen, C.E. Dessent, *J Phys Chem A,* 2013, **117,** 12590-12600.

Figure legends

Fig. 1. (A) Structure of esculetin. (B) Interaction of esculetin with Ct-DNA using UV-visible spectroscopy. UV-visible absorption spectra of esculetin (50 μM) in presence of increasing concentrations of Ct-DNA (0-60 μM) in 10 mM Tris-HCl buffer (pH 7.2). Spectra were recorded in the range of 240-300 nm.

Fig. 2. Interaction of esculetin with Ct-DNA using fluorescence spectroscopy. (A) Fluorescence emission spectra of esculetin (50 μM) in the presence of increasing concentrations of Ct-DNA (0-45μM). Excitation wavelength was 268 nm. Spectra were recorded in the range of 410-560 nm.

Fig. 3. **Stern-Volmer plot for interaction of esculetin with Ct-DNA at three different temperatures**. *Ksv* was calculated from the slope of plot F_0/F vs DNA concentration.

Fig. 4. Modified Stern- Volmer plot. Plot of log$(F_0/F)/F$ *versus* log[Ct-DNA] at different temperatures.

Fig. 5. van't Hoff plot for the interaction of esculetin with Ct-DNA. Plot of log$K$ vs 1/T where K is the binding constant and T is the temperature in Kelvin.

Fig. 6. KI quenching experiment. Stern-Volmer plot F_0/F vs [KI] for fluorescence quenching of esculetin (50μM) by successive addition of KI (0-30 mM) in absence and presence of 50 μM Ct-DNA. Quenching constants were calculated in both the cases. Difference in *Ksv* values was further used to correlate the binding mode of esculetin with DNA.

Fig. 7. Competitive displacement assays. (A) Fluorescence titration of EB-Ct-DNA complex with esculetin. EB-Ct-DNA complex was excited at 476 nm and emission spectra were recorded from 535-675 nm. **(B)** Fluorescence titration of AO-Ct-DNA complex with esculetin. AO-Ct-DNA complex was excited at 480 nm and emission spectra were recorded from 490-600 nm. **(C)** Fluorescence spectra of Hoechst-Ct-DNA complex with esculetin. Hoechst-Ct-DNA complex was excited at 343 nm and emission spectra were recorded from 380-600 nm. **(D)** Stern-Volmer plot for the quenching of fluorescence intensity of different fluorescent dyes-Ct-DNA system by successive addition of esculetin (0-80μM).

Fig. 8. Role of ionic strength. Fluorescence emission intensity plot of esculetin-DNA complex with increasing concentration of NaCl (0-15mM). Excitation wavelength was 268 nm. Fluorescence emission spectra were recorded in the range of 375-575 nm.

Fig. 9. Effect of esculetin on the melting temperature of Ct-DNA. Melting curves of Ct-DNA (50 μM) in absence and presence of esculetin (50 μM), where $A/A_{25°C}$ represents the ratio of absorbance of Ct-DNA with increasing temperature (25-100°C) and absorbance at 25°C.

Fig. 10. Effect of increasing concentration of esculetin on the viscosity of Ct-DNA. Concentration of Ct-DNA was kept constant (50μM) while varying the concentration of esculetin. Data represent mean ± SD of three experiments.

Fig. 11. Effect of esculetin on CD spectra of Ct-DNA. CD spectra of Ct-DNA (30μM) in 10 mM Tris-HCl (pH 7.2) with varying concentration of esculetin. Each spectrum was obtained at 25°C with a 10 mm path length cell.

Fig. 12. Molecular docked structures of esculetin complexed with DNA. **(A)** and **(B)** Surface representation showing minor groove binding of esculetin with dodecamer duplex sequence $d(CGCGAATTCGCG)_2$ (PDB ID: 1BNA). **(C)** Stereoview of the docked conformation of esculetin-DNA complex showing the possibility of hydrogen bonds. The relative binding energy of the complex system was found to be -3.6 kcal/mol.

Tables

Table 1. Various binding constants and thermodynamics parameters calculated at different temperatures for esculetin-DNA interaction.

T (K)	*Ksv* ($\times 10^4$) (M^{-1})	K_q ($\times 10^{12}$) ($M^{-1}s^{-1}$)	*K* ($\times 10^4$) (M^{-1})	*n*	R^2	ΔH (kcal/mol)	ΔS (cal/mol/K)	ΔG (kcal/mol)
294	1.87	1.87	4.49	1.09	0.99979			-6.27
304	1.28	1.28	3.82	1.11	0.99986	-3.77	8.51	-6.35
318	0.72	0.72	2.77	1.13	0.99992			-6.47

R is the correlation coefficient

Table 2. Comparison of *Ksv* values for the quenching of fluorescence intensity by displacement of different fluorescent dyes from Ct-DNA by esculetin.

Dye	*Ksv* (M^{-1})	R[a]	S.D.[b]
EB	1.15×10^3	0.99874	0.7238
AO	0.74×10^3	0.99741	0.7035
Hoechst	5.38×10^3	0.99921	0.7830

[a]R is the correlation coefficient. [b]S.D. is standard deviation.

Figures

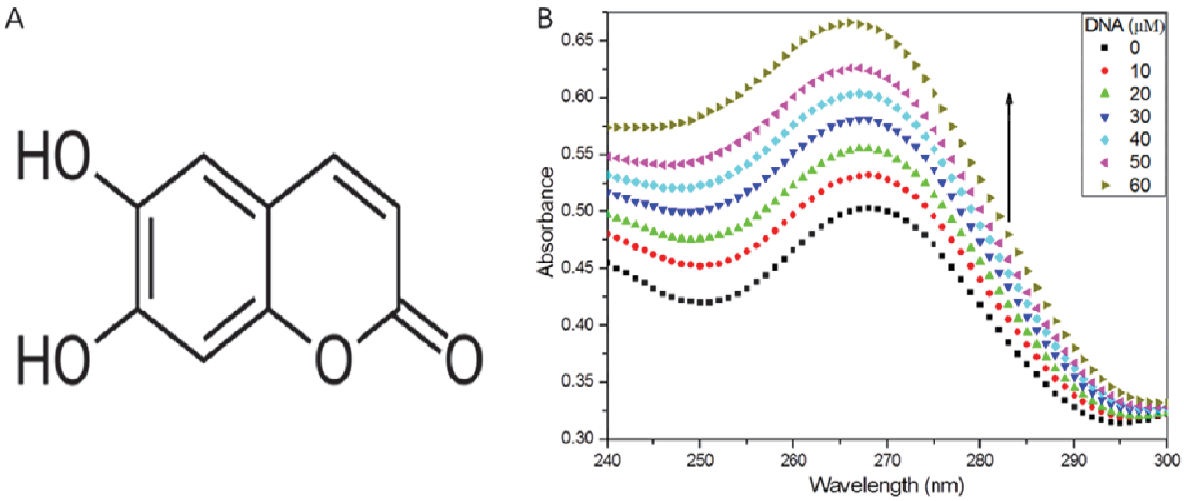

Fig. 1.

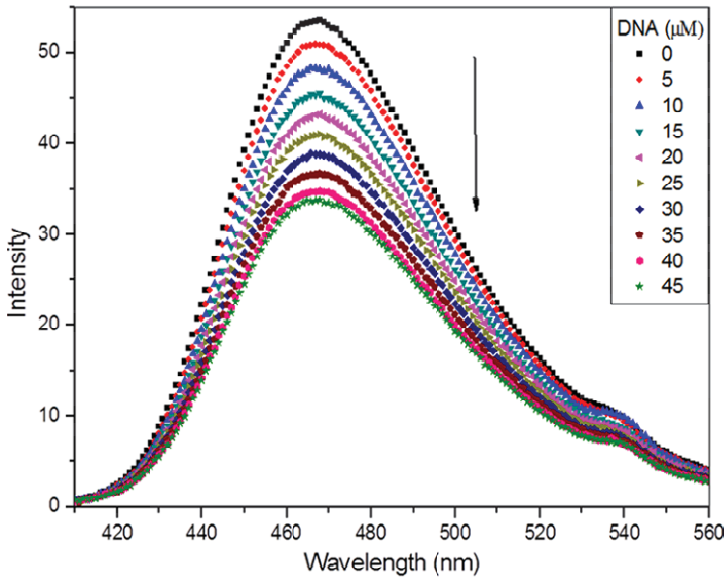

Fig. 2.

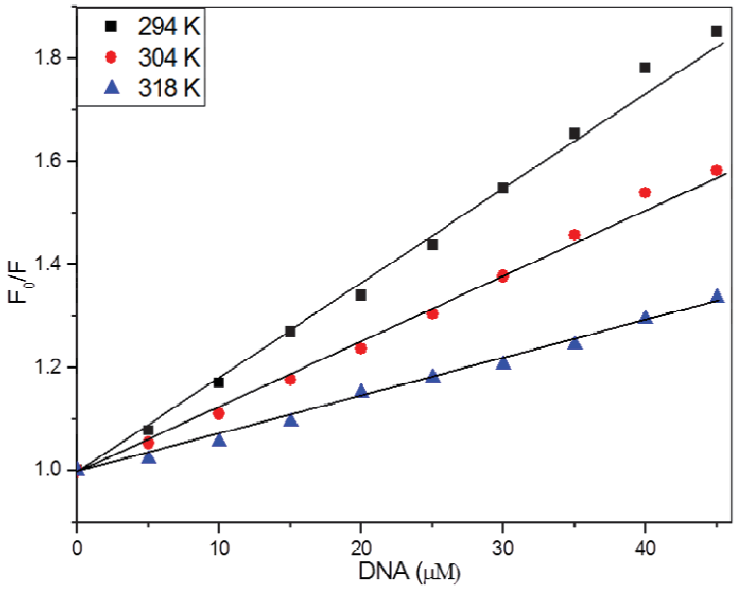

Fig. 3.

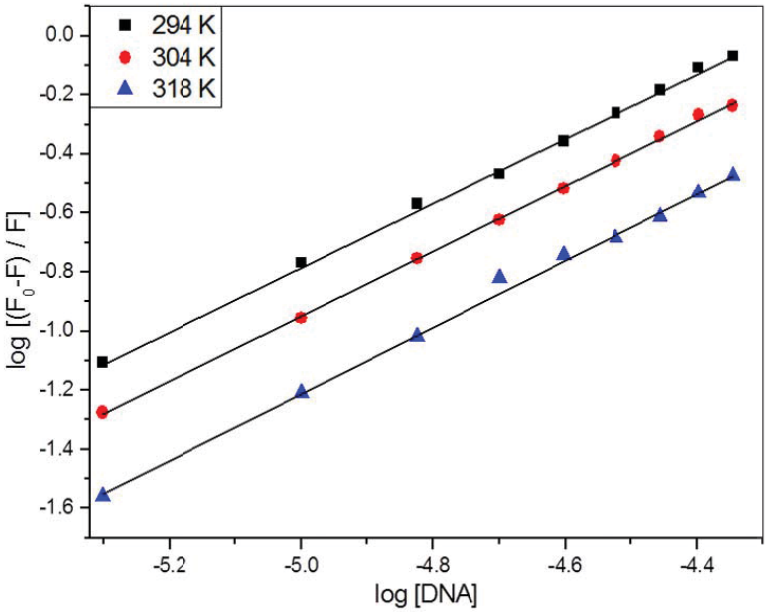

Fig. 4.

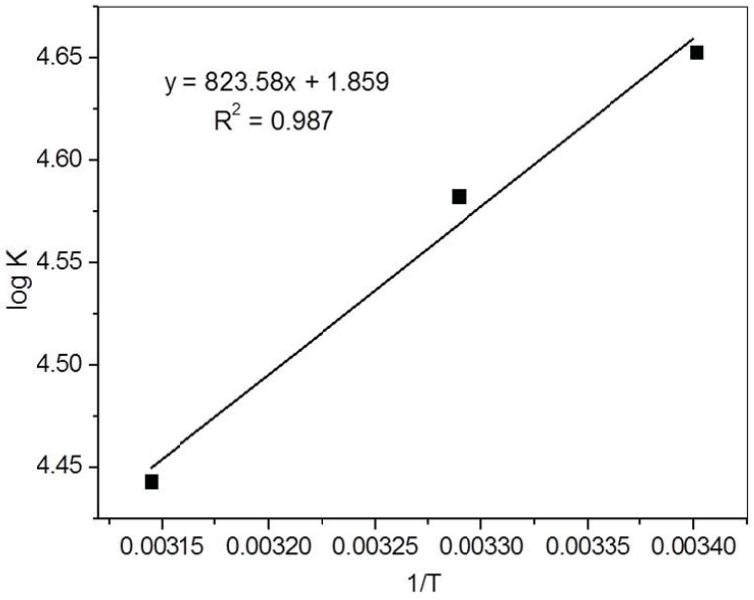

Fig. 5.

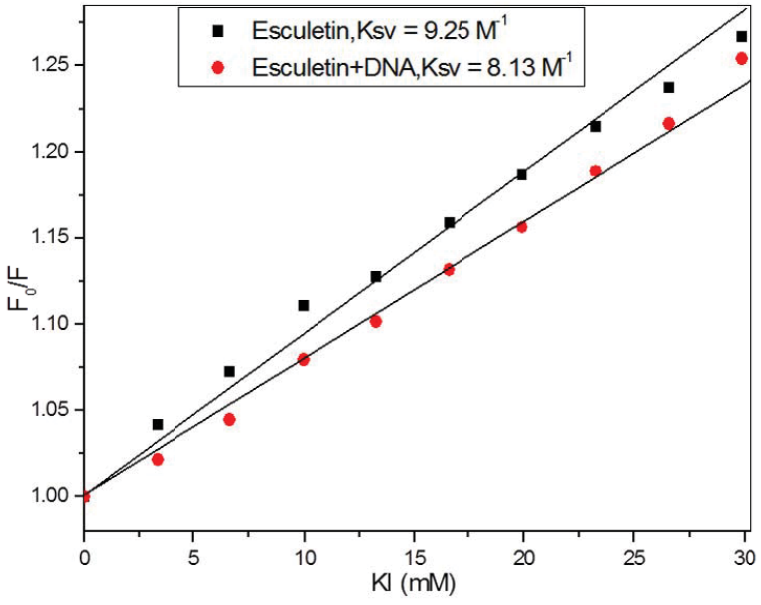

Fig. 6.

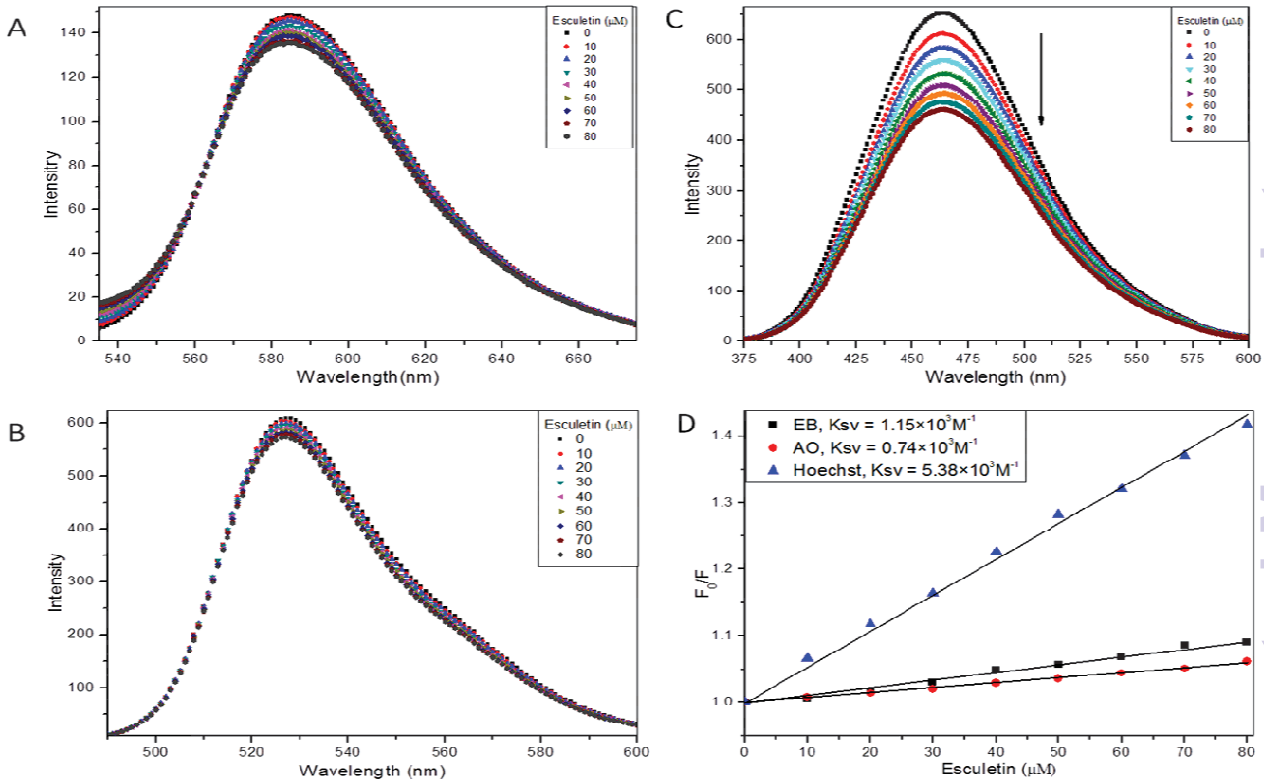

Fig. 7.

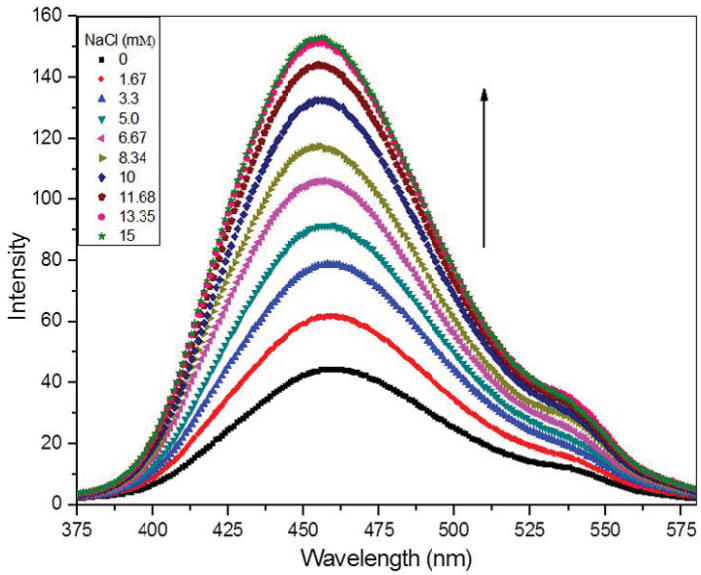

Fig. 8.

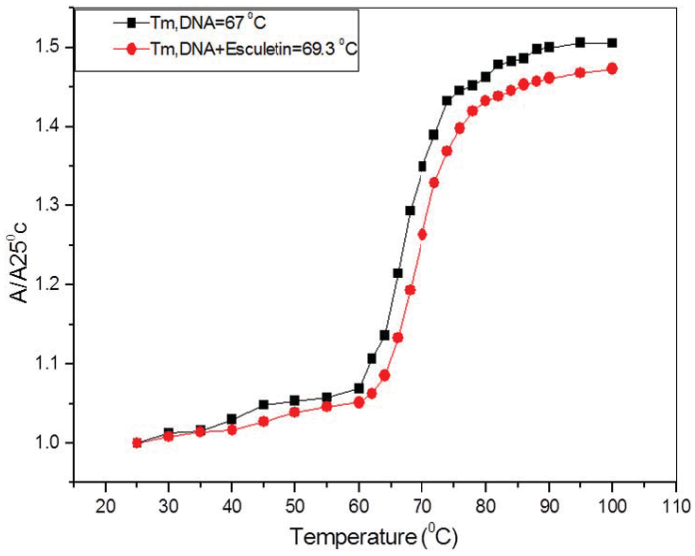

Fig. 9.

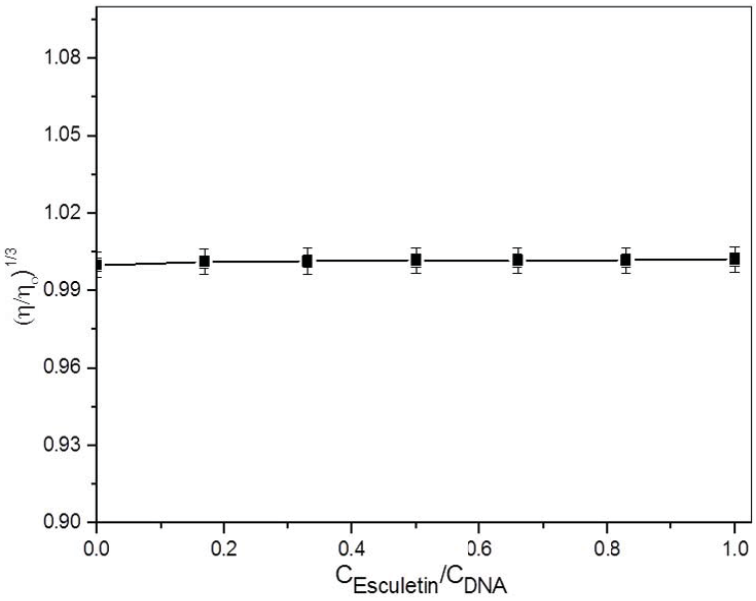

Fig. 10.

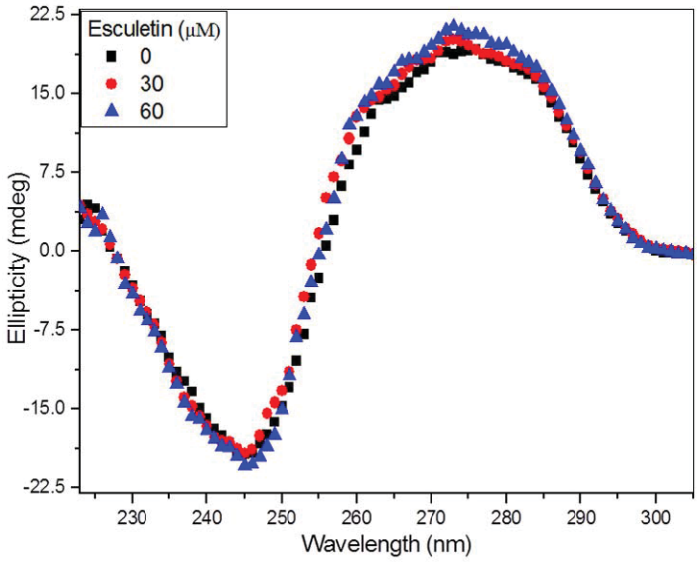

Fig. 11.

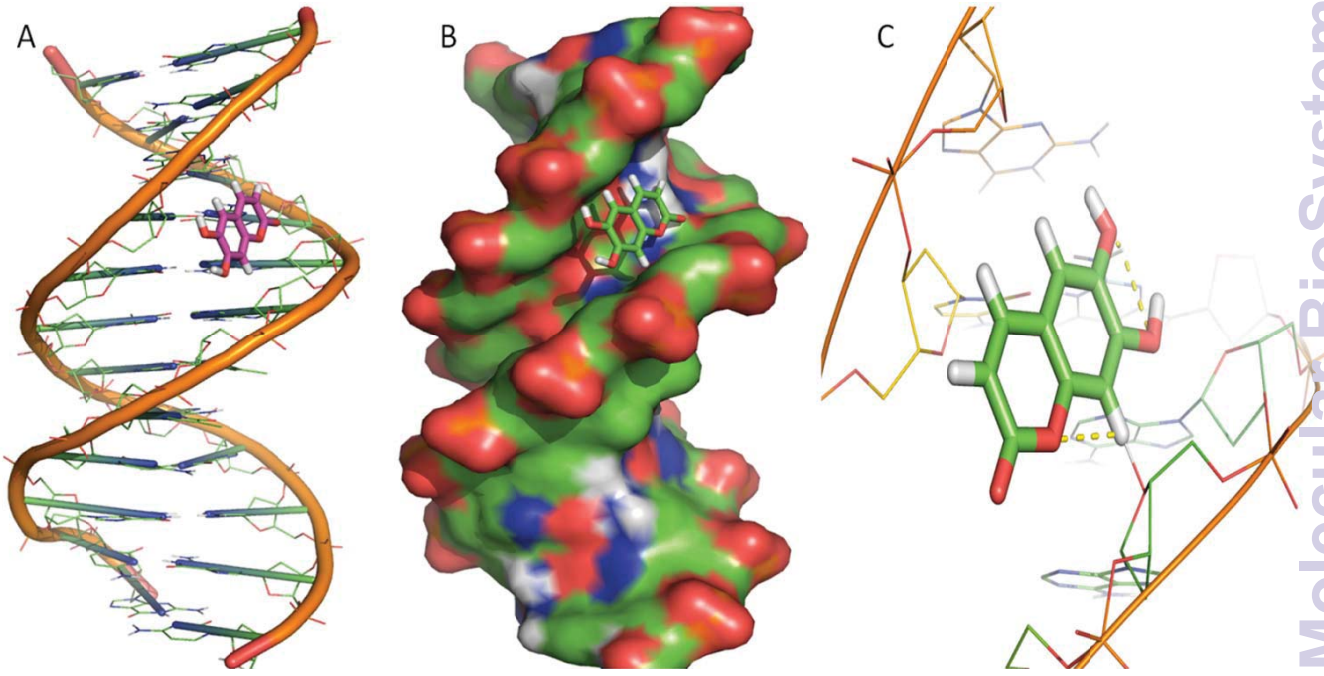

Fig. 12.